Contrib Mineral Petrol (2011) 162:289–302
DOI 10.1007/s00410-010-0597-9

ORIGINAL PAPER

Characterising modal metasomatic processes in young continental lithospheric mantle: a microsampling isotopic and trace element study on xenoliths from the Middle Atlas Mountains, Morocco

Jacqueline Malarkey · Nadine Wittig · D. Graham Pearson · Jon P. Davidson

Received: 4 November 2009 / Accepted: 16 November 2010 / Published online: 12 December 2010

Abstract Clinopyroxene is a major host for lithophile elements in the mantle lithosphere, and therefore it is critical whether we are to understand the constraints that this mineral puts on mantle evolution and melt generation. This study presents a detailed in situ trace element and Sr isotope study of clinopyroxene, amphibole and melt from two spinel lherzolites from the Middle Atlas Mountains, Morocco. The results show that there is limited, but discernable, Sr isotopic variation between clinopyroxene crystals within these xenoliths [$^{87}Sr/^{86}Sr$ ranging from 0.703416 (±11 2SE) to 0.703681 (±12 2SE)]. Trace element patterns show similar interelement fractionation with LREE enrichment, but there is a considerable range in terms of elemental concentration (e.g. over 100 ppm in Sr concentrations). Observed modal clinopyroxene is far more abundant than that predicted from estimates of melt depletion. This along with isotope and trace element variability found in these xenoliths supports a multistage metasomatic process in which clinopyroxene and amphibole are recent secondary additions to the lithospheric mantle. Elemental systematics indicate that the metasomatic mineral assemblage has most recently equilibrated with a carbonatitic melt prior to inclusion in the host basalt. The clinopyroxene from this study is typical of global off-craton clinopyroxene in terms of Sr isotope composition, suggesting that the majority of clinopyroxene in off-craton settings may have a recent metasomatic origin. These findings indicate that caution is required when using peridotite xenoliths to estimate the degree of elemental enrichment in the subcontinental lithosphere.

Keywords Metasomatism · Clinopyroxene · Rb–Sr · Middle Atlas · Mantle xenoliths

Communicated by J. Blundy.

Electronic supplementary material The online version of this article (doi:10.1007/s00410-010-0597-9) contains supplementary material, which is available to authorized users.

J. Malarkey (✉) · N. Wittig · D. Graham Pearson · J. P. Davidson
Northern Centre for Elemental and Isotopic Tracing, Department of Earth Sciences, Durham University, Science Labs, Durham DH1 3LE, UK
e-mail: jacqueline.malarkey@gmail.com

N. Wittig
Friedrich-Alexander Universitaet Erlangen, GeoZentrum Nordbayern, Lithosphere Dynamics, Schlossgarten, 5, 91054 Erlangen, Germany

N. Wittig
Department of Earth, Ocean, and Atmospheric Science, and National High Magnetic Field Laboratory, Florida State University, 1800 E. Paul Dirac Drive, Tallahassee, FL 32310, USA

Introduction

Modal metasomatism, or the addition of new mineral phases by a melt or fluid, has long been the accepted origin for the more exotic phases, such as amphibole and apatite, found in mantle peridotite xenoliths from both on- and off-craton settings (Menzies and Hawkesworth 1987). The more modally abundant mantle minerals olivine, orthopyroxene, clinopyroxene and spinel or garnet were thought to be generally of primary origin, remaining after the initial melt extraction that occurred during lithosphere formation. Clinopyroxene is an important mineral phase in the lithospheric mantle as it is the major host for incompatible elements, such as Sr and REE and therefore exerts a dominant control on the long-term distribution of lithophile

isotopes such as Hf, Sr and Nd. The timing of clinopyroxene addition has significant implications for how long the SCLM has been a relatively fertile source in terms of its geochemical composition. Recent studies have suggested that the majority of clinopyroxene found in mantle xenoliths from on-craton settings may have a metasomatic origin (Gregoire et al. 2003; Pearson et al. 2003; Pearson and Nowell 2002; Simon et al. 2003, 2007; van Achterbergh et al. 2001). The addition of clinopyroxene and other metasomatic phases has generally been linked to kimberlite or proto-kimberlite activity and is therefore considered to predominantly affect on-craton lithospheric mantle. Therefore, the evidence for metasomatic origin of clinopyroxene is profuse in on-craton lithospheric mantle.

Clinopyroxene is also found, often in abundance, in a wide range of mantle xenoliths from off-craton continental settings. The majority of this clinopyroxene is enriched in light REE (rare earth elements), which is inconsistent with melt depletion. To characterise and understand the origin of clinopyroxene in off-craton peridotitic lithosphere, we have selected two spinel peridotite xenoliths from the Middle Atlas Mountains in Morocco, which are thought to be relatively representative of off-craton lithospheric mantle. It is samples such as these that are often used to estimate the composition of primitive upper mantle (PUM), and therefore understanding the effects of refertilisation on these samples is critical to better understanding PUM estimates. The issue of metasomatism and its relation to clinopyroxene in off-craton settings has been investigated by many authors from a trace element perspective (e.g., Menzies 1987; McDonough 1990; Witt-Eickschen and Harte 1994). This study extends this approach to in situ variations in Sr isotopes, coupled with major and trace elements. The desire to approach this problem from an isotopic perspective is driven by models of intraplate volcanism that invoke regions that have been 'enriched' by input from the subcontinental lithospheric mantle (SCLM; McKenzie and O'Nions 1983).

There are a range of possible methods that can be used to investigate in situ trace element and Sr isotope variations in low Rb phases such as clinopyroxene. The method chosen here, which allows the analysis of trace element concentrations and Sr isotope ratios for the same spot, is microdrilling followed by high-precision TIMS (for Sr isotope ratios) and ICP-MS (for trace element concentrations) analysis. This method has a number of benefits over LA-MC-ICP-MS, which is often applied to this type of analysis. The first is that sample preparation and analysis via TIMS minimises isobaric interferences and provides a larger Sr ion signal, allowing smaller differences in Sr isotope composition to be resolved than via LA-ICP-MS (Davidson et al. 2001). This allows samples containing as little as 1 ng of Sr to be analysed without compromising precision and accuracy. The analyses of amphibole and melt that we present would not be possible using LA-MC-ICP-MS due to these phases having higher Rb/Sr ratios. It is also possible, using aliquotting techniques, to measure trace element concentrations, as well as isotope ratios, for the same drilled sample. If LA-MC-ICP-MS were used, then these different analyses would almost certainly have to be carried out on two adjacent spots. This study therefore presents the first microdrilling study of clinopyroxene from mantle xenoliths. The data generated are used to infer a metasomatic origin for the clinopyroxene in the studied samples. A metasomatic origin is suggested to be common for clinopyroxene in worldwide off-craton peridotite xenoliths and supports the view that SCLM is not necessarily a potential long-term source for incompatible element enriched magmas.

Samples

Geological background

A suite of peridotite xenoliths were collected from a single maar in the Azrou Volcanic Field, Middle Atlas Mountains, Morocco. They were erupted approximately 2 Ma in a basaltic host that forms part of the intraplate volcanism in the Middle Atlas Mountains (Duggen et al. 2003; Wittig et al. 2008). The Middle Atlas Mountains represent a failed, inverted rift system that, since 45 Ma, has been affected by the Africa-Europe collision (Duggen et al. 2003). As a result of this collision it has been suggested that there has been delamination of the subcontinental lithospheric mantle (SCLM) beneath the Atlas Mountains as indicated by the high heat flow, gravity and geoid anomalies (Missenard et al. 2006; Teixell et al. 2005; Urchulutegui et al. 2006). The western part of this mountain chain is thought to have significantly thinner lithosphere (60–80 km) than typical NW African lithosphere (130–160 km; Duggen et al. 2009; Missenard et al. 2006; Teixell et al. 2005; Urchulutegui et al. 2006).

Petrography

The peridotite xenoliths collected from the Middle Atlas, Morocco, are coarse-grained, equi-granular spinel lherzolites and harzburgites (Wittig 2006; Wittig et al. 2010a, b). Two spinel lherzolites, 3U and 3V, were chosen for this study as they contained relatively abundant (7 and 14%, respectively; Wittig et al. 2010a), large (2–5 mm), fresh clinopyroxene which is ideal for microdrilling. The major minerals in these samples are olivine (Mg# 89; Mg# = (Mg/(Fe + Mg))*100), orthopyroxene, clinopyroxene and spinel; although the xenoliths also contain

minor amounts of amphibole. The peridotites show a high degree of textural equilibration with no apparent fabric or alignment among the minerals. The mineral phases are subhedral, with rounded edges on some of the clinopyroxene crystals, and although there are cracks within some crystals, there is only limited evidence of secondary alteration (probably containing a product of hydrous alterations such as serpentine or chlorite) along some of the larger cracks.

Both of the xenoliths selected for this study contain quenched melt in 1–5 mm 'pockets' as well as narrow veins along some grain boundaries. The melt pockets appear to represent preferential incongruent melting of amphibole, as indicated by rounded and resorbed residual amphibole within the centre of a melt pocket. In some cases, spinel is observed in the centre of the melt pockets. Some melting of clinopyroxene is also evident from resorbtion of grain edges, but there is no textural evidence of orthopyroxene and olivine contributing to the melt. A small number of primary clinopyroxene crystals, especially those close to melt pockets, have discrete 'spongy' rims that are packed with melt inclusions. The high density of these melts inclusions together with the previously mentioned resorbtion of clinopyroxene suggests that the rim textures represent the effects of partial melting. A second generation of clinopyroxene and spinel microlites has also crystallised from the melt pockets. This late clinopyroxene was too small to be sampled during this study and will not be discussed further. The petrographic evidence indicates that melting is occurring in situ in response to decompression, as there is no evidence of any new minerals, such as feldspar crystallising, that would be expected if the host basalt had invaded at crustal pressures.

Method

The clinopyroxene, olivine and orthopyroxene were all analysed for major and minor elements by wavelength dispersive spectroscopy using a Cameca SX100 Electronprobe microanalyser at the Department of Earth Sciences, University of Cambridge, UK. A beam voltage of 15 kV and a current of 10 nA for the major elements and 100 nA for the minor elements with a beam size of 1 μm were applied. The amphibole was analysed for major and minor elements by wavelength dispersion using a JEOL 733 SuperProbe microprobe at the analytical facility of the School of Geography, Environment and Earth Sciences at Victoria University of Wellington, New Zealand, with a spot beam of ~1 μm at 15 kV and 20 nA.

For trace element and Sr isotope determinations, the clinopyroxene crystals were sampled using two methods: in situ microdrilling and, for comparison, individual fragments of clinopyroxene bounded by fracture planes were picked from a crushed hand sample. In sample 3V, nine clinopyroxene fragments ranging from 70 to 28 μg were handpicked from a clean clinopyroxene fraction. These samples were rinsed in 18 mΩ MilliQ water (MQ) in a sonic bath for 10 min repeatedly, changing the MQ each time, until the MQ was devoid of particles. The clinopyroxene chips were then leached in 6M UpA HCl at in a warm ultrasonic bath for 30 min before a final MQ rinse.

The in situ microdrilling was carried out on 100-μm-thick sections of the bulk xenolith following the procedure outlined in Charlier et al. (2006), using a New Wave MicroMill at the Northern Centre for Elemental and Isotopic Tracing (NCIET), Durham University, UK. The resulting drilled holes are conical with a diameter of approximately 50 μm and a drilling dept ranging between 60 and 70 μm. Over 20 clinopyroxene crystals were sampled from one thick section of 3V (Fig. 1) and 9 crystals from a thick section of 3U. Only the cores of the crystals were drilled, avoiding any potential contamination along cracks or grain boundaries. The drilled powder was collected in MQ, dried down and weighed to allow accurate determination of trace element concentrations. The drilled weights varied from 5 to 218 μg. Repeated weighing of the same mass, in the range used here, gave a reproducibility of less than 0.1 μg ($n = 60$).

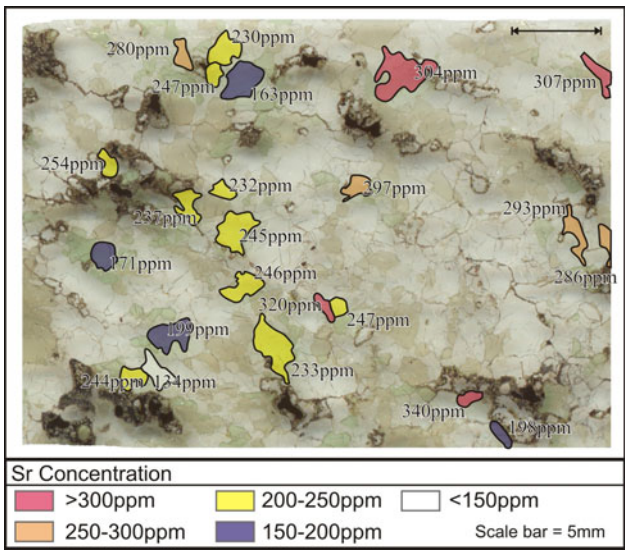

Fig. 1 A scanned image of the 100-μm-thick section of xenolith 3V used in the drilling campaign. The coloured crystals represent clinopyroxene crystals that were drilled and the shading represents the Sr concentration with the lowest values in purple and the highest in *red*. The absolute values are labelled adjacent to the clinopyroxene crystals. Extensive melt pockets are shown as *dark brown*. There are adjacent crystals with a difference in Sr concentration exceeding 100 ppm. The distance between the cores of these crystals is, in some case, less than 0.5 cm

Both the drilled powders and picked fragments were processed using micro-Sr dissolution (150 µl 29M HF + 50 µl of 16M HNO_3 followed by 200 µl 12M HCl followed 200 µl 16M HNO_3, drying down between each step) and purification chemistry (Charlier et al. 2006) A 10% aliquot, by mass, was taken for trace element analysis, and the remaining 90% was processed through micro-Sr columns using cleaned Sr-spec resin (Charlier et al. 2006). Romil triple distilled "UpA" grade acids were used throughout.

Sr isotope ratios were measured using a ThermoScientific Triton TIMS at NCIET, Durham University, UK. The samples were loaded onto Re filaments using a TaF_5 activator. The analysis consisted of 180 ratios with an integration time of 4 s per ratio. Over the period of this study, the $^{87}Sr/^{86}Sr$ reproducibility of 3 ng loads of the NBS987 standard ($n = 25$, yielding beam sizes that are typical of the smaller samples sizes analysed here) yielded an $^{87}Sr/^{86}Sr$ of 0.710237 (±16 2sd). Sample values were normalised to a standard value of $^{87}Sr/^{86}Sr$ 0.710240 (Thirlwall 1991). All samples were corrected for blank contribution. The mass of Sr analysed varied from 6 to 30 ng in the drilled samples and up to 100 ng in the picked chips. The average total procedural Sr blank was 11 pg (±14 2sd, $n = 8$), which is considerably less than 1% of the analysed Sr. The blank correction, therefore, was less than the internal run uncertainties.

The trace element aliquot was diluted using 480 µl of UpA 0.05M HNO_3 and analysed for 21 trace elements using a ThermoElectron Element II ICPMS at Durham University, UK, calibrated relative to internationally recognised standards (W2, AGV-1, BHVO-1). Details of this procedure including the drift and reproducibility can be found in Malarkey (2010). A sample of W2 diluted to an appropriate signal size and run with the samples gives a reproducibility of less than 10% (Malarkey 2010). The parameters used were similar to those used in Font et al. (2007). Accuracy and repeatability of the trace element concentrations using the aliquotting technique are 10% or better and are given in Harlou et al. (2009).

Results

Clinopyroxene and amphibole major element composition

The clinopyroxene from the peridotites is diopside with a Mg# of 89 and a Cr# (Cr# = (Cr/(Cr + Al))*100) of 9 in 3U and 8 in 3V. These compositions are typical of relatively young continental lithospheric mantle (Pearson et al. 2003). There is remarkably little variation in major element composition among the clinopyroxene crystals in either sample. Despite the textural difference between cores and rims of clinopyroxene, there is no consistent major element zoning or discrete compositional differences.

Amphibole is present as inclusions in both 3V and 3U and as a relict crystal in a melt pocket in 3U. The amphibole data are taken from Wittig et al. (2006). The inclusion in 3V has an average Mg# of 86.7, whereas in 3U it is 88.4. The relict amphibole in 3U, on the other hand, has a Mg# of 86.7. There is some zoning observed in the amphibole inclusion in 3U with the rims showing lower Cr and Al contents and higher Ti.

Trace element and Sr isotope results

The major, trace element and Sr isotope data are presented in the Supplementary Dataset.

Clinopyroxene

In situ analysis allows the detailed studies of intergrain and intragrain variation to be examined for trace elements as well as Sr isotopes for the same spot. In both samples, a considerable range in trace element concentrations is observed among individual crystals, including adjacent grains. Sr concentrations range from 134 to over 300 ppm in 3V (Fig. 1) and from 218 to over 300 ppm in 3U. However, despite this large intergrain variation, the within-grain variation was much less, and trace element concentrations from the same crystal are within 10% of each other. There is also a range in Rb concentrations from less than 0.01 to 0.7 ppm. This is comparable to ranges found in bulk clinopyroxene separates from other off-craton suites (Downes 1987). The large range in clinopyroxene trace element concentrations does not correlate with any textural or spatial parameters such as crystal size, location or proximity to other phases (including melt). However, it should be noted that it is not possible to fully constrain the three-dimensional setting of the grains using a single two-dimensional thin section. Similar trace element variation among clinopyroxene crystals in individual peridotite xenoliths has been observed using LA-ICP-MS (e.g. Ionov et al. 2002a; Schmidberger et al. 2003).

REE patterns for the Middle Atlas clinopyroxene (Fig. 2) from the two xenoliths are very similar with $(Ce/Yb)_N$ ratios (all ratios are normalised to PM; McDonough and Sun 1995) ranging from 5 to 10.4 for 3V ($n = 33$) and from 6.1 to 11.4 for 3U ($n = 7$). The larger range for 3V can be attributed to a larger sample set. There are differences in $(La/Ce)_N$ ratios between the two xenoliths, which has been reported before (Wittig et al. 2008, 2010a). In 3V, the average $(La/Ce)_N$ ratio is 0.7 compared with 1.2 in 3U (Fig. 2b). The variation in trace element concentrations between the picked fragments and the drilled clinopyroxene

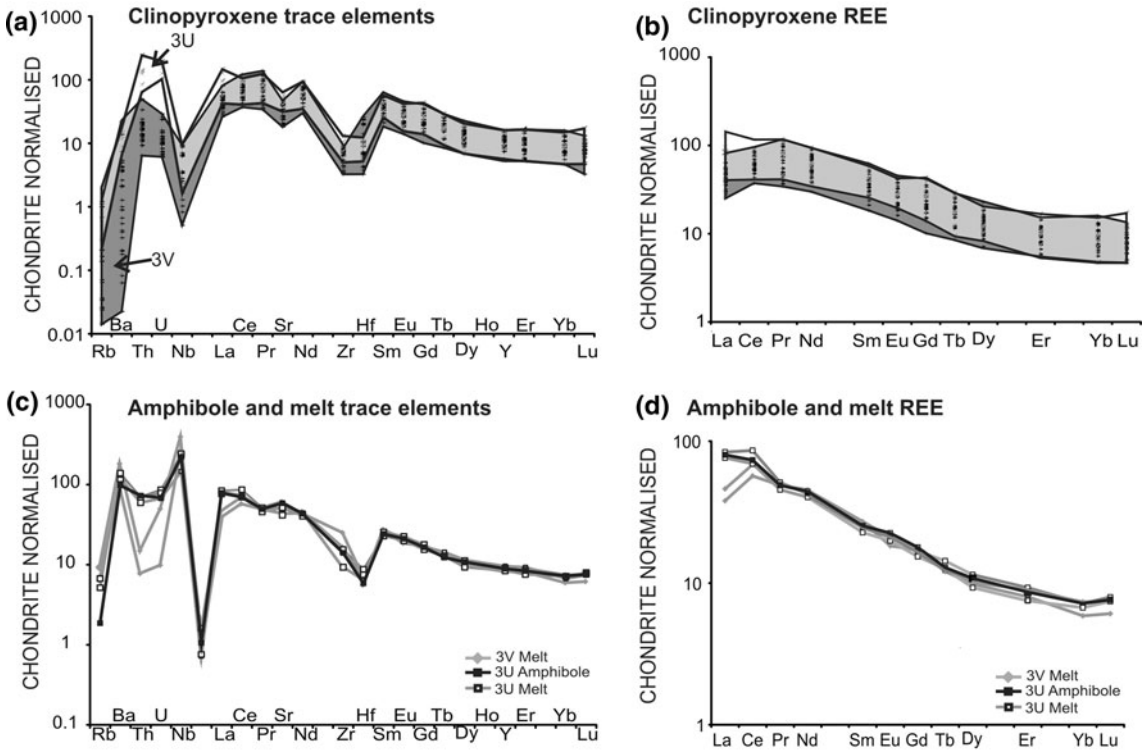

Fig. 2 **a** Primitive mantle normalised (McDonough and Sun 1995) trace elements patterns for the drilled and picked clinopyroxene samples from xenoliths 3U (*paler shading*) and 3V (*darker shading*). **b** Chondrite normalised (McDonough and Sun 1995) REE patterns for the clinopyroxene from 3U (*paler shading*) and 3V (*darker shading*). **c** Primitive mantle normalised (McDonough and Sun 1995) trace element patterns for the one amphibole crystal from 3U (*black*) and melt drilled from both 3U (*black*, *open squares*) and 3V (*grey diamonds*). **d** Chondrite normalised (McDonough and Sun 1995) REE patterns for one amphibole crystal from 3U (*black*) and melt drilled from the both 3U (*black*, *open squares*) and 3V (*grey diamonds*)

crystals is similar; although due to the larger sample size, the range in the picked sample is smaller.

Complete multielement patterns are, like the REE patterns, relatively similar (Fig. 2a). However, there are distinct differences in the most incompatible end of the spectrum, especially for Th and U concentrations that are distinctly higher in the clinopyroxene from 3U (average Th concentration in 3V is 0.56 ppm compared with 4.2 ppm in 3U). Rb concentrations are also higher in 3U which results in higher Rb/Sr ratios for 3U compared with 3V.

The clinopyroxene from the Atlas xenoliths shows a range in $^{87}Rb/^{86}Sr$ from <0.001 to 0.018, which is typical of mantle diopside (e.g. Pearson et al. 2003). Downes et al. (1987), for example, observed a range in $^{87}Rb/^{86}Sr$ for bulk clinopyroxene separates from peridotite xenoliths of the Massif-Central region of <0.001 to 0.047. The range in $^{87}Rb/^{86}Sr$ observed in the clinopyroxene from the Atlas samples does not show any correlation with other trace element concentrations or ratios or textural occurrence.

The Atlas peridotite clinopyroxene analysed here show much more limited initial Sr isotope ($^{87}Sr/^{86}Sr_i$) variation (Fig. 3) than clinopyroxene from oceanic and cratonic lithospheric mantle xenoliths reported in LA-MC-ICP-MS studies (Neumann et al. 2004; Schmidberger et al. 2003, respectively). The $^{87}Sr/^{86}Sr_i$ for the Atlas clinopyroxene, both picked and drilled, ranges from 0.703416 (±11 2SE) to 0.703681 (±12 2SE). This range is considerably less than those observed from comparable microdrilling studies of clinopyroxene from on-craton peridotites (Fig. 4; Malarkey 2010; Malarkey et al. 2008). Previous LA-MC-ICP-MS studies such as those carried out by Schmidberger et al. (2003) observed a range in $^{87}Sr/^{86}Sr_i$ of 0.00079 from 0.70442 (±6 2SE) to 0.70521 (±10 2SE) in clinopyroxene from a single mantle xenolith (sample NK 2–3) from the on-craton Somerset Island kimberlite.

The drilled clinopyroxene shows similar $^{87}Sr/^{86}Sr$ systematics to the picked chips although the picked crystals show a smaller range in isotopic composition, possibly due to fewer clinopyroxene crystals being sampled (9 picked chips compared with 19 drilled clinopyroxene crystals). In sample 3V, two clinopyroxene grains were drilled twice to look for any heterogeneity within grains, but the results are within uncertainty of each other. This is consistent with the lack of major and trace element zoning in the clinopyroxene. There are no correlations between the limited Sr isotope variability in the Atlas clinopyroxene and other

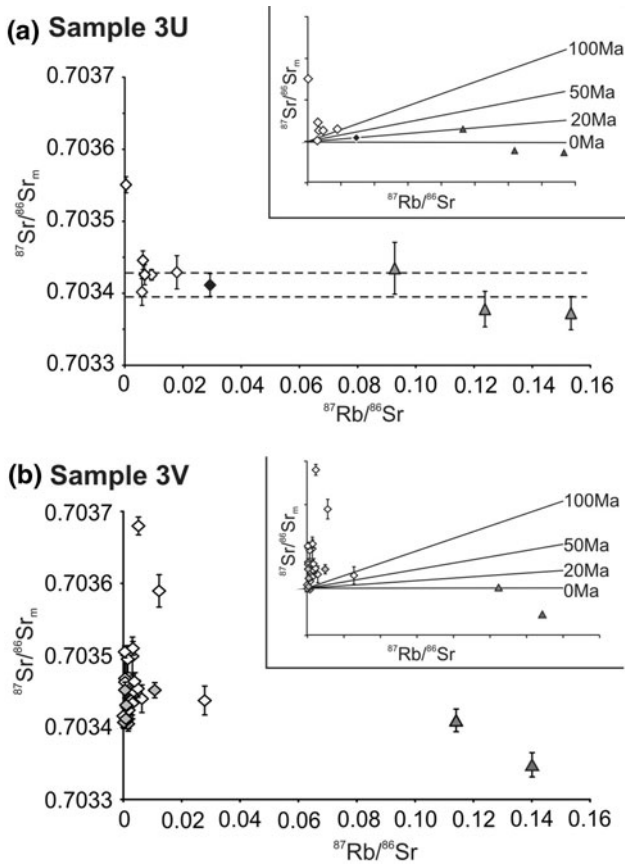

Fig. 3 **a** An isochron plot of $^{87}Rb/^{86}Sr$ against $^{87}Sr/^{86}Sr_m$ for the drilled clinopyroxene (*white diamonds*), amphibole (*black diamonds*) and melt (*grey triangles*) from 3U. The *error bars* represent 2SE, where *no error bars* are seen; the symbol is larger than the uncertainty. **b** An isochron plot of $^{87}Rb/^{86}Sr$ against $^{87}Sr/^{86}Sr_m$ for the drilled clinopyroxene (*white diamonds*), picked clinopyroxene (*grey diamonds*) and drilled melt (*grey triangle*). The *error bars* represent 2SE. The *insets* illustrate reference isochrons plotted to illustrate the range in $^{87}Sr/^{86}Sr$ that can be generated through radiogenic ingrowth

trace element concentrations or ratios, including $(La/Ce)_N$ (which varies between the two xenoliths).

In order to assess how secondary alteration may affect the Sr isotope value of a clinopyroxene crystal, this was sampled by drilling along the cracks lined with alteration (possibly serpentine or chlorite) and compared with a crack-free region of the same crystal. The drilled cracks were found to have a much more radiogenic $^{87}Sr/^{86}Sr_i$ value of 0.705644 (±19 2SE) compared to 0.703416 (±11 2SE) for the fresh clinopyroxene. Therefore, the range in $^{87}Sr/^{86}Sr_i$ observed in the Atlas clinopyroxene could, in principle, be explained by addition of about 4% 'crack alteration' to the least radiogenic clinopyroxene crystal. However, this is unlikely to be the explanation for the following reasons. The leaching procedure applied to the handpicked clinopyroxene efficiently removes such contamination, and these samples yield Sr isotope systematics identical to the microdrilled clinopyroxene. In addition, great care was taken to avoid such cracks and alteration along the cracks is relatively uncommon.

The microsampled Atlas clinopyroxene can be compared to analyses of bulk clinopyroxene separates from peridotite xenoliths from similar off-craton intraplate settings. Such mineral separates give an average value for the whole xenolith, but given the lack of previous in situ studies on these types of samples, these are the only data that can be used for comparison. The Middle Atlas clinopyroxene have a similar average $^{87}Sr/^{86}Sr_i$ value relative to $^{87}Sr/^{86}Sr_i$ values from other off-craton clinopyroxene ($^{87}Sr/^{86}Sr_i$ 0.7035, see Fig 8 for references).

Amphibole and melt

A rounded amphibole crystal from the centre of a melt pocket in xenolith 3U was drilled and analysed for trace elements and Sr isotopes along with the surrounding melt. A number of other melt pockets from xenoliths, 3V and 3U, were also analysed. In 3U the trace element patterns of the melt and the amphibole essentially overlap (Fig. 2c). The REE patterns in both the melt [$(La/Yb)_N = 10.8$] and the amphibole [$(La/Yb)_N = 10.9$] show are similar to those of the clinopyroxene [$(La/Yb)_N$ mean = 9.5 for 3U, Fig. 2d]. The most prominent deviation from the clinopyroxene pattern is a positive Nb anomaly in the trace element patterns from both the melt and the amphibole. This is reflected in the $(U/Nb)_N$ ratio which, for 3U, is 0.31 and 0.32 in the amphibole and melt, respectively, compared with a mean of 91 for the clinopyroxene. The amphibole and melt also have higher Rb and Ba concentrations than the clinopyroxene, as expected from relative partition coefficients (Ionov et al. 2002a).

The melt analysed from 3V, where there was no amphibole remaining for comparison, shows a similar trace element pattern to the amphibole and melt from 3U (Fig. 2c). There is evidence that there was amphibole present in 3V before melting took place as the melt has a positive Nb anomaly. The melt in 3V shows the same characteristically lower $(La/Ce)_N$ ratios and lower Th and U concentrations that are seen in the clinopyroxene in 3V compared with 3U.

The amphibole crystal from 3U yielded an initial $^{87}Sr/^{86}Sr$ ratio of 0.703413 (±16 2SE). This value plots towards the lower end of the range in Sr isotopes observed in the clinopyroxene from 3U but is within error of four out of the six clinopyroxene crystals analysed (Fig. 3a). The amphibole $^{87}Sr/^{86}Sr_i$ value also overlaps with the value obtained for the melt surrounding the amphibole crystal (0.703431 ± 36 2SE). The three samples of melt analysed from 3U are, as a group, slightly less radiogenic in terms of $^{87}Sr/^{86}Sr_i$ than the clinopyroxene but do overlap the least

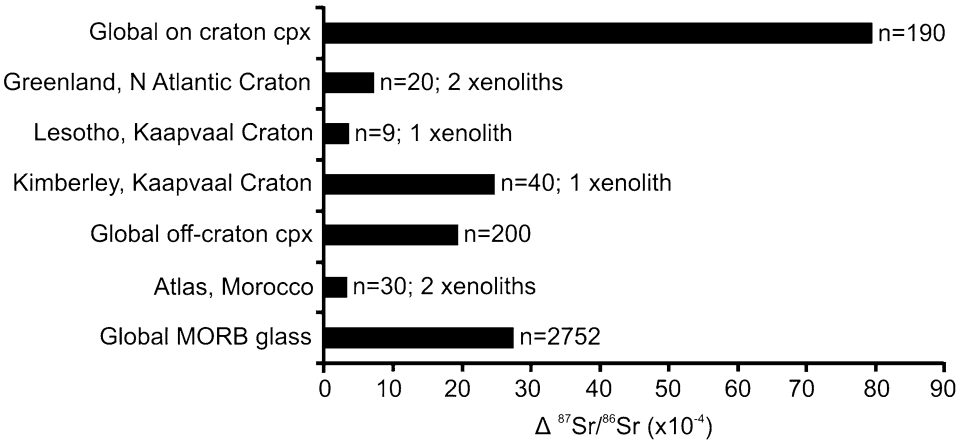

Fig. 4 The range in $^{87}Sr/^{86}Sr$ (expressed as the difference between the highest and lowest value; labelled as $\Delta^{87}Sr/^{86}Sr$) observed in a range of clinopyroxene databases. The global on- and off-craton databases use bulk clinopyroxene mineral separate data, whereas the clinopyroxene from Greenland, Lesotho, Kimberley and the Atlas Mountains (this study) is from drilled clinopyroxene. The global MORB database is from GERM. On- and off-craton data sourced from Ionov et al. (2002a), Downes et al. (2003), Downes and Dupuy (1987), Stosch and Lugmair (1986), Witt-Eickschen et al. (2003), Menzies (1988), Porcelli et al. (1992), Roden et al. (1988), Deng and Macdougall (1992), Cohen et al. (1984), Xu et al. (2008), Choi et al. (2008), Tang and Chen (2008), Ionov et al. (2006), Pearson et al. (1995), Schmidberger et al. (2001, 2002, 2003), Carlson et al. (2004), Bedini et al. (2004), Macdougall and Haggerty (1999), Richardson et al. (1985), Erlank et al. (1987), Simon et al. (2003, 2007)

radiogenic clinopyroxene. This is the same in the two melt samples analysed from 3V. There was no corresponding amphibole remaining in 3V, but a clinopyroxene within a melt pocket gave an $^{87}Sr/^{86}Sr_i$ of 0.703544 (±20 2SE), whereas the surrounding melt was significantly less radiogenic ($^{87}Sr/^{86}Sr_i = 0.703348 \pm 17$ 2SE). The melt from both Atlas xenoliths shows a range in $^{87}Sr/^{86}Sr_i$ from 0.703348 (±17 2SE) to 0.703431 (±36 2SE), significantly less radiogenic than the majority of the clinopyroxene from the two samples.

Discussion

Melting history

Melt depletion

In order to assess the origin of the clinopyroxene in the Middle Atlas peridotites, it is important to first understand the melting history of the SCLM. In cratonic settings, the lithospheric mantle is thought to have experienced 30–40% melt extraction (Boyd 1989; Pearson and Wittig 2008), which is well above the 23% melting required to exhaust clinopyroxene from the resitite (Walter 1998). However, in off-craton settings the degree of melt extraction is much more difficult to constrain because extents of melting appear smaller, and the response of major elements may be more subtle (Ionov and Hofmann 2007). Wittig et al. (2010a, b) have studied the melting history of the suite of peridotite xenoliths from the Middle Atlas, including the two samples studied here. The whole rock FeO and MgO contents, traditionally used to estimate the extent of melt removal and depths of initial melting, plot approximately along a 2-GPa melting residue trend with melt extraction estimates ranging from 5 to 25%. However, other parameters show a more complicated picture. The whole rock SiO_2 and Al_2O_3 compositions project away from the melting trend and towards amphibole and spinel-pyroxene, indicating that there has been considerable modal metasomatic addition of these phases. This therefore brings into question the validity of using whole rock major elements to quantify melt removal (see Wittig et al. 2010a for an extended discussion of this issue).

Trace elements, especially the REE, can also be used to further constrain the melting history. The effect of such partial melting on clinopyroxene in a peridotite host has been modelled (Hellebrand et al. 2002) and compared with the REE patterns from the Atlas samples. The trace element composition of a clinopyroxene from a fertile spinel lherzolite from the Vitim Basalt Field, Russia, (Ionov 2004) with a similar whole rock trace element composition to primitive mantle was used as the starting composition. Progressive fractional melting was modelled, starting at 3GPa (but within the spinel field), and the changing trace element composition of the clinopyroxene was calculated as the melt fraction increased (an example of a clinopyroxene remaining after 10% melt extraction is shown in Fig. 5). The results show that, as expected, the LREE become progressively depleted relative to the heavy REE resulting in REE patterns that are more reminiscent of clinopyroxene from Type 1A lherzolite xenoliths (Pearson

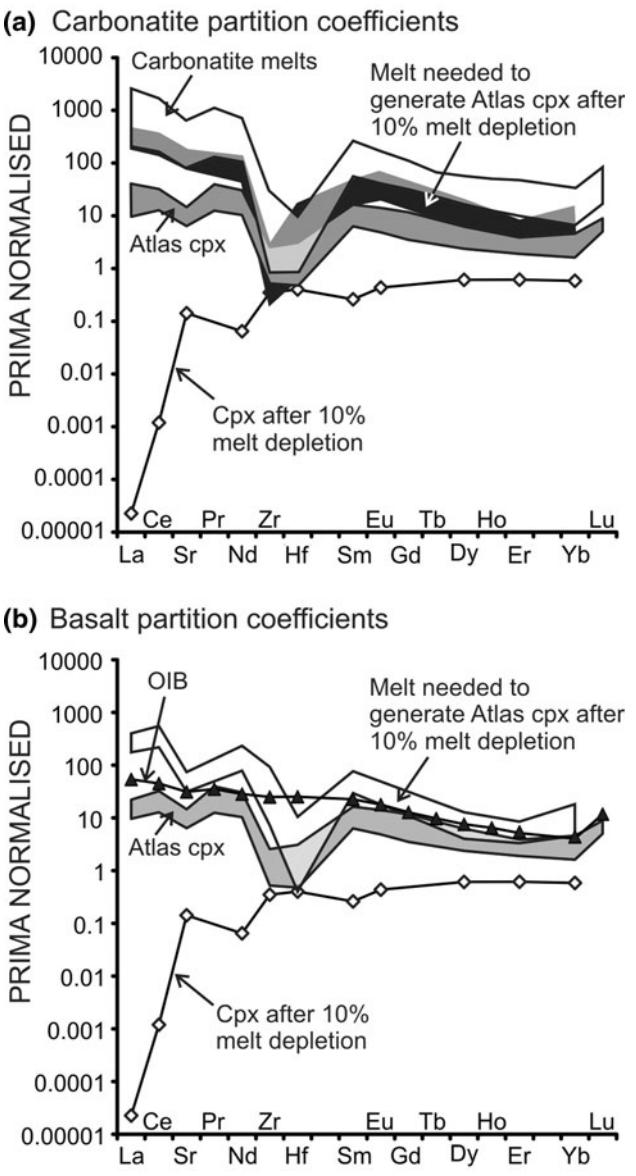

Fig. 5 PRIMA normalised (McDonough and Sun 1995) modelling of a clinopyroxene starting with sample 313-15 (Ionov et al. 2002a) and extracting 10% melt (see text for details; Hellebrand et al. 2002). **a** Metasomatic melt required to generate the Atlas clinopyroxene from the residual clinopyroxene is modelling using clinopyroxene-melt carbonatite partition coefficients (Adam and Green 2001; Blundy and Dalton 2000; Klemme et al. 2002a). A range of carbonatite melts are also shown (Bizimis et al. 2003) for comparison. **b** Metasomatic melt required to generate the Atlas clinopyroxene from the residual clinopyroxene is modelling using clinopyroxene-basalt partition coefficients (Blundy and Dalton 2000; Hauri and Hart 1994). Typical OIB is shown for comparison (McDonough and Sun 1995)

et al. 2003). This is in contrast to the REE patterns from the Atlas clinopyroxene which show relative LREE/HREE enrichment consistent with crystallisation from a metasomatic melt that postdates the melt depletion event that formed the lithosphere (Frey and Green 1974; Ionov et al. 2002a).

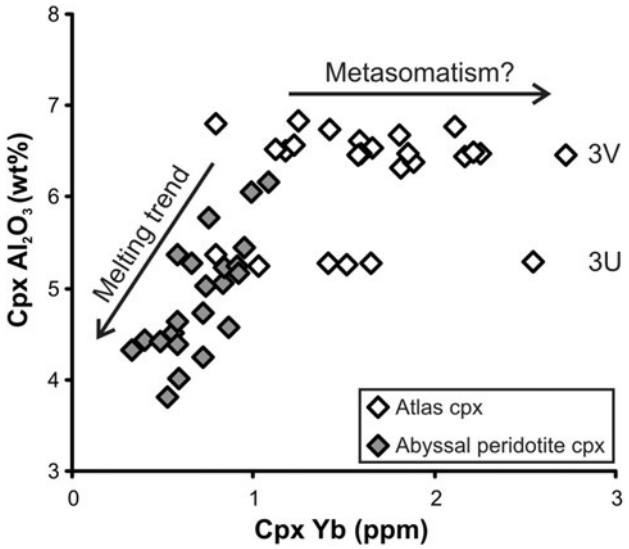

Fig. 6 Plot of clinopyroxene Al_2O_3 (wt%) against Yb concentration (ppm) showing abyssal peridotite data that show a clear melting trend (Hellebrand et al. 2002) against data from the Atlas clinopyroxene. The clinopyroxene from the abyssal peridotites represents analyses from individual samples, whereas the Atlas data are individual clinopyroxene analyses from two samples. The *upper array* of Atlas clinopyroxene are data from sample 3V and the *lower array* from sample 3U

The HREE, which are less affected by metasomatism, may provide some information about the degree of melt extraction from the lithosphere. Canil (2004), for example, used whole rock Yb to constrain melting history, arguing that it is robust to most metasomatic melts, and it has been shown to be useful in cratonic peridotites. Wittig et al. (2010b) have shown that only one xenolith in the extended Atlas suite records shallow melting up to about 20% using Lu in clinopyroxene alone. This conclusion is supported by the study of Raffone et al. (2009) who used a correlation between decreasing Yb concentrations in clinopyroxene with increasing olivine Mg number in a different suite of peridotite xenoliths from the Middle Atlas to assess the degree of melting. They concluded, using clinopyroxene Yb concentrations, combined with modal clinopyroxene contents, that the lithosphere experienced about 20% melting. However, there are other factors to consider; the decrease in modal clinopyroxene, for example, could be attributed to melt-peridotite reactions and Yb, although relatively robust to metasomatic affects, these cannot be ruled out (Raffone et al. 2009). The Atlas samples presented here show elevated Yb concentrations, compared to a depleted clinopyroxene, as seen from the trace element modelling (Fig. 5). In order to examine this further, Yb concentrations have been plotted against Al_2O_3 in the clinopyroxene and compared to clear melting trends observed in abyssal peridotites (Fig. 6; Hellebrand et al. 2002). The two Atlas samples show horizontal arrays

plotting away from the melting trend, although the low Yb clinopyroxene crystals from the Atlas peridotites do overlap with the fertile end of the abyssal peridotite spectrum. Clearly, these data are not a reliable tool to estimate melt depletion. In summary, it is difficult to constrain the degree of melt extraction for the Middle Atlas lithosphere as the effects of metasomatism have overprinted the geochemical proxies. Furthermore, it is unlikely that the currently observed 14% clinopyroxene would be remaining after the removal of up to 20% melt (Walter 1998), implying that clinopyroxene and amphibole are metasomatic additions.

Recent remelting

The most recent event in the melting history of these peridotites is expressed petrographically as melt pockets containing quenched melt with secondary microlites of clinopyroxene and spinel. These melt pockets could be either the result of melt infiltration from the host basalt or they could represent in situ decompressional melting related to emplacement. The latter is favoured here as the melt pockets do not contain any new minerals, such as plagioclase, that might be indicative of an infiltrating melt. This is further supported by the location of the melt pockets that are centred on the most fusible minerals, such as amphibole and clinopyroxene. The lack of plagioclase also implies that the melting is occurring at depth in the spinel facies. Only one amphibole crystal was observed (in 3U), found within a melt pocket. This crystal shows a resorbtion texture, with rounded edges and a high concentration of melt inclusions around the rim. These textures were also observed in the clinopyroxene crystals rimming the melt pockets. The petrography therefore suggests that the melt pockets represent in situ melting of the peridotite during emplacement, as seen in some other off-craton peridotite xenoliths (Ionov et al. 1994; Yaxley et al. 1997).

The melt analysed from both xenoliths shows a similar trace element pattern to the amphibole, with a characteristic positive Nb and Ba anomalies. Although the trace element signatures in the melt patches are also similar to the clinopyroxene, these positive Nb and Ba anomalies suggest that the majority of the melt has a significant amphibole component.

The Sr isotope data also support in situ melting where the melt is dominated by rapid batch melting of the amphibole. In 3U, both an amphibole crystal and the surrounding glass were drilled, and the resulting $^{87}Sr/^{86}Sr_i$ values are within uncertainty of each other. In 3V, a clinopyroxene and the adjacent melt were drilled, and the Sr isotope ratios were significantly different at 0.703550 and 0.703358, respectively. This, with the trace element evidence puts forward a strong case for the melt pockets representing rapid, in situ melting of amphibole where this mineral and the melt have not equilibrated.

Nature of the metasomatism in the Middle Atlas

The presence of 14% clinopyroxene in 3V is inconsistent with a residual origin for the clinopyroxene, indicating that the clinopyroxene, and probably the amphibole, has been added by a metasomatic event. This is further supported by the trace element patterns recorded in the clinopyroxene from the Middle Atlas which are light REE enriched, relative to the heavy REE. This would indicate that either the clinopyroxene has a metasomatic origin or at the very least has been overprinted by a metasomatic melt. Trace element patterns and ratios are tools that can be used to characterise metasomatic melts although care must be taken as reactive flow models have shown that trace element ratios can be fractionated by this process (Ionov et al. 2002a). The modelling of Ionov et al. (2002a), however, does not fractionate Hf or Zr while generating a similar spectrum of REE patterns as seen in the Atlas clinopyroxene. The negative anomaly for these elements observed in the multielement plots is therefore indicative of clinopyroxene that has crystallised from, or re-equilibrated with, a carbonate melt (Blundy and Dalton 2000). The metasomatic melt that would be required to generate the trace element patterns observed in the Atlas clinopyroxene from a residual clinopyroxene (depleted by 10% melt extraction as a conservative estimate) has been modelled (Fig. 5; Hellebrand et al. 2002 used for melt depletion modelling). The predicted metasomatic melt needed to produce the trace element systematics observed in the Atlas clinopyroxene was generated using carbonatite-clinopyroxene partition coefficients (Fig. 5a; Adam and Green 2001; Blundy and Dalton 2000; Klemme et al. 2002b) and basalt-clinopyroxene partition coefficients (Fig. 5b; Blundy and Dalton 2000; Hauri and Hart 1994). The results of this modelling show that the melt that generated the Atlas clinopyroxene had a negative Zr-Hf anomaly which is observed in the carbonatite melts. Although the range of basaltic melts that would be required depends on partition coefficients, the patterns are jagged and do not reflect basaltic melts. The addition of a carbonatite melt is therefore the most likely candidate for the most recent metasomatic event as the predicted melts approximately match a range of carbonatites (Bizimis et al. 2003). This is also supported by Wittig et al. (2010b) and by the presence of carbonatite magmatism in the Middle Atlas (Woolley 2002), indicating that these melts are present in the lithospheric mantle. However, this is not an exact match which could be attributed to a number of factors. For example, pre-existing clinopyroxene may have experienced and recorded metasomatism with various reagents, and equilibration of this clinopyroxene with a

carbonatite may result in slightly atypical trace element systematics now observed. Similarly, it is likely that there is some discrepancy between erupted carbonatites and the carbonatite melt at depth (Foley et al. 2009).

Ionov et al. (2002a) numerically modelled porous reactive flow of a metasomatic melt away from a vein in order to explain trace element variations observed in a suite of spinel xenoliths from Spitsbergen in response to the changing mineralogy of the peridotite, which ultimately results in fractionated light REE (Fig. 7). The trace elements in the Middle Atlas clinopyroxene are similar to those observed in the Spitsbergen Type 2 clinopyroxene that were modelled to be close to a melt vein (Fig. 7; Ionov et al. 2002a). This would suggest that either the clinopyroxene precipitated in the Middle Atlas xenoliths was close to a melt channel/source or that the metasomatism was significantly advanced such that a wide zone had re-equilibrated with the melt. However, there are differences in the $(La/Ce)_N$ ratios between 3V (0.42–0.80) and 3U (0.98–1.4), which may record some evidence of reactive flow processes. In the Spitsbergen xenoliths, there is a considerable range in $(La/Ce)_N$ from 0.92 to 3.59 as the melt becomes progressively fractionated away from the vein (Ionov et al. 2002a). These differences are larger for the La/Ce than any other ratio of adjacent REE, and therefore these variations are the last to be equilibrated by continued metasomatism. This would therefore imply that 3U was maybe slightly further from the melt source and experienced a marginally more fractionated melt than 3V. This is consistent with the scenario proposed by Raffone et al. (2009) that these xenoliths had sampled the rejuvenated lithosphere close to the dunitic channels that represent relict metasomatic melt channels.

Sr isotopes are not fractionated by processes such as reactive flow although a mixing scenario with the metasomatic agent having a significantly different Sr isotope ratio relative to the depleted host may be proposed in a zone at the metasomatic front (Ionov et al. 2002b). However, in the Atlas samples the Sr isotopes show very limited variation, and there is no observed correlation between $^{87}Sr/^{86}Sr$ and trace elements, including Sr, which would indicate a mixing relationship. This implies the carbonatite melt has dominated the Sr isotope composition of the clinopyroxene.

Timing of metasomatism

Time constraints from Sr isotopes

The timing of this initial melt depletion event has been difficult to constrain using Re–Os isotopes due to the extensive metasomatic overprinting (Wittig et al. 2008). The lithophile budget in peridotites is dominated by any metasomatic effects, and therefore it may be possible to date metasomatic events using Rb–Sr or Sm–Nd isotope systems (e.g. Erlank et al. 1987). There is a sufficient range in Rb/Sr in the Moroccan clinopyroxene to generate isotopic variation well outside the analytical error (Fig. 3). However, the Rb–Sr data from the Middle Atlas clinopyroxene does not show an isochronous relationship (Fig. 3), and therefore it is not possible to accurately date the clinopyroxene addition using the Rb–Sr isochron technique. It is possible to plot reference isochrons through the clinopyroxene data, but this does not yield any information (Fig. 3). The range in clinopyroxene $^{87}Sr/^{86}Sr$ is therefore not generated by radiogenic ingrowth but probably the

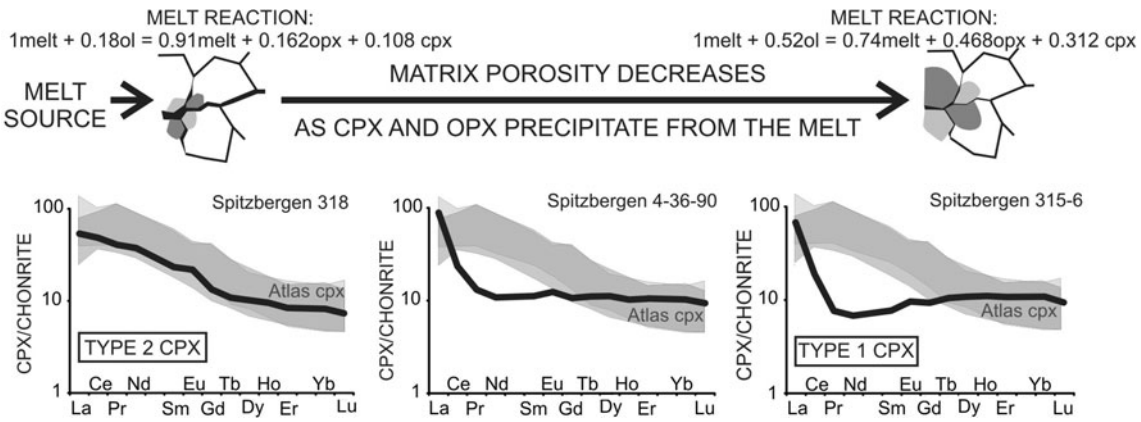

Fig. 7 A schematic representation to illustrate Ionov's (2002) model for percolative fractional crystallisation where trace element concentration in clinopyroxene varies with distance from the melt source. The melt source is at the *left* of the diagram and as the melt moves away from the melt vein clinopyroxene and opx precipitate from the melt and the remaining melt evolves. This leads to the change in REE pattern observed on the left with the clinopyroxene crystallising closest to the melt at the *bottom* of the diagram. The *black patterns* are representative analyses from the Spitsbergen clinopyroxene samples that match the model predictions for each stage. The *grey shaded* area represents the clinopyroxene REE patterns analysed from the Atlas xenoliths

result of complex metasomatic interactions, and this holds true for the majority of mantle clinopyroxene Rb/Sr (lithophile) isotope data available from off-craton SCLM to date (Pearson et al. 2003).

Time constraints from trace element distributions

It is possible to use other approaches to evaluate the timing of metasomatism. The Atlas samples show a considerable range in trace element concentrations between clinopyroxene crystals within the two xenoliths. In 3V, for example, there are two touching clinopyroxene crystals that differ in Sr content by about 80% (100 ppm difference). These variations show that diffusive equilibration has not been attained. The time over which diffusion would even out such differences between adjacent clinopyroxene crystals can be approximated using Fick's Law ($x = \sqrt{Dt}$ where x is the diffusion distance, t is the time, and D is the diffusion coefficient) if the diffusion coefficients are known. Diffusion models have shown that Sr should equilibrate at the grain size scale in mantle peridotites over periods of 1–100 Myr at lithospheric temperatures and pressures (Sneeringer et al. 1984). This timescale is strongly dependant on temperature and is further reduced by the presence of melt along grain boundaries. If a distance (x) of 0.2 cm, as observed in the thin section, is taken between the cores of the adjacent crystals (calculated at 1,000°C; Sneeringer et al. 1984), then the time for complete equilibration for Sr would be approximately 2.5 Ma. It is likely therefore that the variation of 100 ppm in Sr concentrations, which represents significant disequilibrium, would persist for more than 2 or 3 Myr before entrainment into the basalt. This timescale is supported by Wittig et al. (2010b) who argue, using Pb isotopes, that the most recent metasomatism could not have occurred more than 20 Ma. This constraint argues for a relatively recent metasomatic event that coincides with the intraplate volcanism that has sampled the continental mantle root although these clinopyroxenes and their host volcanic rocks have distinctly different Pb isotopes (Wittig et al. 2010b).

Global implications

The Sr isotopic composition of the clinopyroxene from the Middle Atlas xenoliths is typical of clinopyroxene from similar off-craton settings (e.g. Baker et al. 1998; Bedini and Bodinier 1999). A probability density function (PDF) has been plotted for a global compilation of off-craton clinopyroxene data ($n = 205$) from published mineral separate data with the Atlas clinopyroxene marked for comparison (Fig. 8). The $^{87}Sr/^{86}Sr$ mode for off-craton clinopyroxene is approximately 0.7035, which is similar to the average for the Atlas samples, 0.70346 and also within the range observed for present-day OIBs (McDonough and Sun 1995). However, this plot shows that the range in $^{87}Sr/^{86}Sr$ in most off-craton settings is limited and that therefore the metasomatic origin concludes for the clinopyroxene from the Middle Atlas may be common to many other off-craton peridotites. The narrow range and sharp peak observed in the Sr distribution would be incompatible with a range of ancient metasomatic melts and therefore indicates that the majority of off-craton clinopyroxene has been recently overprinted by the convecting mantle. This is further confirmed by a PDF plot of off-craton clinopyroxene $^{143}Nd/^{144}Nd$ data, again form bulk clinopyroxene separate data. The PDF plot has a mode at $^{143}Nd/^{144}Nd$ of 0.5126 which is close to present-day bulk earth values ($^{143}Nd/^{144}Nd = 0.51264$; Rollinson 1993). If these clinopyroxene crystals were residual, with Sm/Nd ratios higher than bulk earth, then the clinopyroxene would have

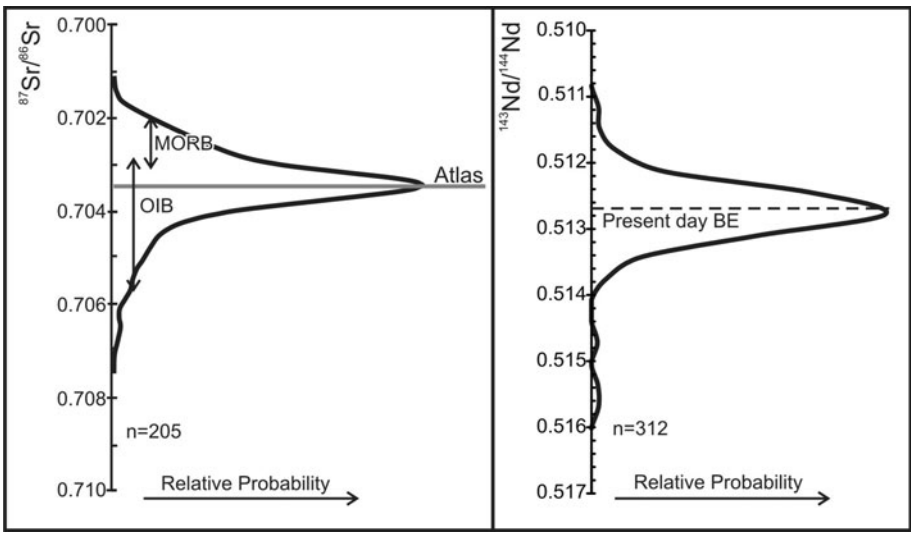

Fig. 8 PDF (probability density function) plots of global off-craton clinopyroxene $^{87}Sr/^{86}Sr$ and $^{143}Nd/^{144}Nd$ data from mineral separates. The range of $^{87}Sr/^{86}Sr$ for MORB and OIB are shown as are the Atlas data (*grey line*). The present-day bulk earth $^{143}Nd/^{144}Nd$ is also shown. Data taken from Ionov et al. (2002a), Downes et al. (2003), Downes and Dupuy (1987), Stosch and Lugmair (1986), Witt-Eickschen et al. (2003), Menzies (1988), Porcelli et al. (1992), Roden et al. (1988), Deng and Macdougall (1992), Cohen et al. (1984)

considerably more radiogenic $^{143}Nd/^{144}Nd$ ratios than bulk earth. Alternatively, if the clinopyroxene had formed from an ancient enriched metasomatic melt, with Sm/Nd ratios lower than bulk earth, then the clinopyroxene would have considerably less radiogenic $^{143}Nd/^{144}Nd$. Therefore, the coincidence of clinopyroxene Nd isotope ratios with present-day bulk earth is inconsistent with long-term enrichment or depletion in the lithosphere. However, it should be stressed again that this may reflect a recent overprint, and it is not possible to use Nd or Sr to 'see though' the most recent metasomatic event.

The global database therefore suggests that clinopyroxene may be a recent addition to much of the non-cratonic lithosphere. Clinopyroxene, in off-craton lithosphere, is an important host for incompatible elements, and therefore the modal abundance and timing of clinopyroxene addition exercise a strong control on the relative fertility of the lithosphere. The recent addition of clinopyroxene to the lithosphere implies that the enriched nature of lithospheric mantle, in both on- and off-craton settings, may only be a recent phenomenon as suggested by (Pearson and Nowell 2002). However, mantle xenoliths have long been known to provide a biased view of the mantle, and therefore this apparent enrichment may not truly represent the bulk mantle (Menzies and Hawkesworth 1987). In peridotite massifs, where it is possible to sample away from metasomatic veins, light REE depleted REE patterns are more common, and these may be more representative of the bulk depleted mantle. In this study, the trace element systematics suggest that the Moroccan xenoliths were located relatively close to melt veins during metasomatic activity, and it likely therefore that it is the vein system being sampled (Bodinier et al. 1988; Menzies and Hawkesworth 1987). If this situation is common then it is likely that the incompatible element abundances in most lithospheric peridotites will consistently overestimate the incompatible abundances in the continental lithospheric mantle (Pearson and Nowell 2002).

The direct sampling of melt that has formed from low degree melting of the amphibole in the Atlas lithosphere, now present as melt pockets in the peridotite, did not generate melts with a wide range of Sr isotopic ratios despite predominantly melting an exotic phase such as amphibole. This would therefore imply that in off-craton settings, where the isotopic variation in the lithosphere is more restricted than in on-craton settings, it is not possible to generate lithospheric melts with very heterogeneous Sr isotopic variation. It then follows that the isotopic diversity observed in off-craton continental basalts—including many flood basalts—cannot reflect a lithospheric mantle source and must either be due to heterogeneity in the convecting mantle or/and crustal contamination.

Conclusions and implications

1. The modal amount of clinopyroxene coupled with the trace element and major element concentrations in the clinopyroxene from these samples are consistent with a metasomatic, as opposed to a residual, origin.
2. The major element composition and mineral chemistry of constituent clinopyroxene crystallised from a recent carbonatitic metasomatic event.
3. The $^{87}Sr/^{86}Sr$ values of clinopyroxene and amphibole in the Middle Atlas peridotites are inconsistent with long-term enrichment or depletion and may be explained by recent crystallisation/re-equilibration with a melt originating in the convecting mantle.
4. PDF plots of a global off-craton database show that the majority of off-craton clinopyroxene has a Sr isotope ratio of $\sim$0.7035 consistent with the above process.
5. Spinel lherzolite xenoliths from off-craton settings, often used in melting experiments, are therefore unlikely to truly represent *primary* fertile mantle if the majority of the clinopyroxene is metasomatic.
6. The incompatible trace element budget of the bulk peridotite, in these spinel facies xenoliths, is dominated by the clinopyroxene. Therefore, the recent addition of clinopyroxene to the SCLM implies that although the SCLM is relatively enriched, now this may not always have been the case.

Acknowledgments This study was supported by a Natural Environment Research Council studentship (NERC/S/A/2006/14005) to JM. The authors would like to thank Geoff Nowell and Chris Ottley for technical assistance. Vikki Martin and Ofra Klein BenDavid are thanked by JM for patiently demonstrating the drilling and chemistry techniques and providing good company during long days in the laboratory. We would like to thank Joel Baker and an anonymous reviewer for constructive reviews which improved the manuscript. Jon Blundy is thanked for his editorial handling of the manuscript.

References

Adam J, Green T (2001) Experimentally determined partition coefficients for minor and trace elements in peridotite minerals and carbonatitic melt, and their relevance to natural carbonatites. Eur J Mineral 13(5):815–827

Baker J, Chazot G, Menzies M, Thirlwall M (1998) Metasomatism of the shallow mantle beneath Yemen by the Afar plume—Implications for mantle plumes, flood volcanism, and intraplate volcanism. Geology 26:432–434

Bedini RM, Bodinier JL (1999) Distribution of incompatible trace elements between the constituents of spinel peridotite xenoliths: ICP-MS data from the east African rift. Geochim Cosmochim Acta 63:3883–3900

Bedini RM, Blichert-Toft J, Boyet M, Albarede F (2004) Isotopic constraints on the cooling of the continental lithosphere. Earth Planet Sci Lett 223(1–2):99–111

Bizimis M, Salters VJM, Dawson JB (2003) The brevity of carbonatite sources in the mantle: evidence from Hf isotopes. Contrib Mineral Petrol 145(3):281–300

Blundy J, Dalton J (2000) Experimental comparison of trace element partitioning between clinopyroxene and melt in carbonate and silicate systems, and implications for mantle metasomatism. Contrib Mineral Petrol 139(3):356–371

Bodinier JL, Dupuy C, Vernieres J (1988) Behavior of trace-elements during upper mantle metasomatism—evidences from the Lherz Massif. Chem Geol 70(1–2):152–152

Boyd FR (1989) Compositional distinction between oceanic and cratonic lithosphere. Earth Planet Sci Lett 96(1–2):15–26

Canil D (2004) Mildly incompatible elements in peridotites and the origins of mantle lithosphere. Lithos 77(1–4):375–393

Carlson RW, Irving AJ, Schulze DJ, Hearn BC (2004) Timing of Precambrian melt depletion and Phanerozoic refertilization events in the lithospheric mantle of the Wyoming Craton and adjacent Central Plains Orogen. Lithos 77(1–4):453–472

Charlier BLA, Ginibre C, Morgan D, Nowell GM, Pearson DG, Davidson JP, Ottley CJ (2006) Methods for the microsampling and high-precision analysis of strontium and rubidium isotopes at single crystal scale for petrological and geochronological applications. Chem Geol 232(3–4):114–133

Choi SH, Mukasa SB, Zhou XH, Xian XH, Androniko AV (2008) Mantle dynamics beneath East Asia constrained by Sr, Nd, Pb and Hf isotopic systematics of ultramafic xenoliths and their host basalts from Hannuoba, North China. Chem Geol 248(1–2): 40–61

Cohen RS, Onions RK, Dawson JB (1984) Isotope geochemistry of xenoliths from East-Africa—implications for development of mantle reservoirs and their interaction. Earth Planet Sci Lett 68(2):209–220

Davidson J, Tepley F, Palacz Z, Meffan-Main S (2001) Magma recharge, contamination and residence times revealed by in situ laser ablation isotopic analysis of feldspar in volcanic rocks. Earth Planet Sci Lett 184(2):427–442

Deng FL, Macdougall JD (1992) Proterozoic depletion of the lithosphere recorded in mantle xenoliths from Inner-Mongolia. Nature 360(6402):333–336

Downes H (1987) Tertiary and quaternary volcanism in the Massif Centrale, France. Geol Soc Spec Publ 30:517–530

Downes H, Dupuy C (1987) Textural, isotopic and Ree variations in spinel peridotite xenoliths, Massif-Central, France. Earth Planet Sci Lett 82(1–2):121–135

Downes H, Reichow MK, Mason PRD, Beard AD, Thirlwall MF (2003) Mantle domains in the lithosphere beneath the French Massif Central: trace element and isotopic evidence from mantle clinopyroxenes. Chem Geol 200(1–2):71–87

Duggen S, Hoernle K, van den Bogaard P, Rupke L, Morgan JP (2003) Deep roots of the Messinian salinity crisis. Nature 422(6932):602–606

Duggen S, Hoernle KA, Hauff F, Klugel A, Bouabdellah M, Thirlwall MF (2009) Flow of Canary mantle plume material through a subcontinental lithospheric corridor beneath Africa to the Mediterranean. Geology 37(3):283–286

Erlank AJ, Waters FG, Hawkesworth CJ, Haggerty SE, Allsopp HL, Menzies MA (1987) Evidence for mantle metasomatism in peridotite nodules from the Kimberley Pipes, South Africa. In: Menzies MA, Hawkesworth C (eds) Mantle metasomatism, vol. Academic Press, London, pp 221–312

Foley SF, Yaxley GM, Rosenthal A, Buhre S, Kiseeva ES, Rapp RP, Jacob DE (2009) The composition of near-solidus melts of peridotite in the presence of CO_2 and H_2O between 40 and 60 kbar. Lithos 112(Supplement 1):274–283

Font L, Nowell GM, Pearson DG, Ottley CJ, Willis SG (2007) Sr isotope analysis of bird feathers by TIMS: a tool to trace bird migration paths and breeding sites. J Anal At Spectrom 22(5):513–522

Frey FA, Green DH (1974) Mineralogy, geochemistry and origin of Ilherzolite inclusions in Victorian basanites. Geochim Cosmochim Acta 38(7):1023–1059

Gregoire M, Bell DR, Le Rouex AP (2003) Garnet lherzolites from the Kaapvaal craton (South Africa): trace element evidence for a metasomatic history. J Petrol 44(4):629–657

Harlou R, Pearson DG, Nowell GM, Ottley CJ, Davidson JP (2009) Combined Sr isotope and trace element analysis of melt inclusions at sub-ng levels using micro-milling, TIMS and ICPMS. Chem Geol 260(3–4):254–268

Hauri EH, Hart SR (1994) Constraints on melt migration from mantle plumes—a trace-element study of peridotite xenoliths from Savaii, Western-Samoa. J Geophys Res-Solid Earth 99(B12): 24301–24321

Hellebrand E, Snow JE, Hoppe P, Hofmann AW (2002) Garnet-field melting and late-stage refertilization in 'residual' abyssal peridotites from the Central Indian Ridge. J Petrol 43(12): 2305–2338

Ionov D (2004) Chemical variations in peridotite xenoliths from Vitim, Siberia: Inferences for REE and Hf behaviour in the garnet-facies upper mantle. J Petrol 45(2):343–367

Ionov DA, Hofmann AW (2007) Depth of formation of subcontinental off-craton peridotites. Earth Planet Sci Lett 261(3–4):620–634

Ionov DA, Hofmann AW, Shimizu N (1994) Metasomatism-induced melting in mantle xenoliths from Mongolia. J Petrol 35(3): 753–785

Ionov DA, Bodinier JL, Mukasa SB, Zanetti A (2002a) Mechanisms and sources of mantle metasomatism: major and trace element compositions of peridotite xenoliths from Spitsbergen in the context of numerical modelling. J Petrol 43(12):2219–2259

Ionov DA, Mukasa SB, Bodinier JL (2002b) Sr-Nd-Pb isotopic compositions of peridotite xenoliths from Spitsbergen: numerical modelling indicates Sr-Nd decoupling in the mantle by melt percolation metasomatism. J Petrol 43(12):2261–2278

Ionov DA, Chazot G, Chauvel C, Merlet C, Bodinier JL (2006) Trace element distribution in peridotite xenoliths from Tok, SE Siberian craton: a record of pervasive, multi-stage metasomatism in shallow refractory mantle. Geochim Cosmochim Acta 70(5):1231–1260

Klemme S, Blundy JD, Wood BJ (2002a) Experimental constraints on major and trace element partitioning during partial melting of eclogite. Geochim Cosmochim Acta 66(17):3109–3123

Klemme S, Blundy JD, Wood BJ (2002b) Some experimental constraints on major and trace element partitioning during partial melting of eclogite. Geochim Cosmochim Acta 66(15A): A405–A405

Macdougall JD, Haggerty SE (1999) Ultradeep xenoliths from African kimberlites: Sr and Nd isotopic compositions suggest complex history. Earth Planet Sci Lett 170(1–2):73–82

Malarkey J (2010) Micro-geochemistry of the mantle and its volcanic rocks. In: Department of Earth Sciences, vol PhD. Durham University, Durham

Malarkey J, Pearson DG, Davidson JP, Wittig N (2008) Origin of Cr-diopside in peridotite xenoliths: recent metasomatic addition revealed by a micro-sampling, trace element and Sr isotopic study of on-craton and off-craton peridotites. In: 9th International kimberlite conference extended abstract volume

McDonough WF, Sun SS (1995) The Composition of the Earth. Chem Geol 120(3–4):223–253

McKenzie D, O'Nions RK (1983) Mantle reservoirs and ocean island basalts. Nature 301:229–231

Menzies MA (1988) The geometry of Archean and Proterozoic lithospheric mantle domains beneath the western USA. Chem Geol 70(1–2):54–54

Menzies MA, Hawkesworth CJ (1987) Mantle metasomatism, vol. Academic Press, London, p xix, 472 p

Missenard Y, Zeyen H, de Lamotte DF, Leturmy P, Petit C, Sebrier M, Saddiqi O (2006) Crustal versus asthenospheric origin of relief of the Atlas Mountains of Morocco. J Geophys Res-Solid Earth 111:B03401

Neumann ER, Griffin WL, Pearson NJ, O'Reilly SY (2004) The evolution of the upper mantle beneath the Canary Islands: information from trace elements and Sr isotope ratios in minerals in mantle xenoliths. J Petrol 45(12):2573–2612

Pearson DG, Nowell GM (2002) The continental lithospheric mantle: characteristics and significance as a mantle reservoir. Philos Trans R Soc Lond Ser Math Phys Eng Sci 360(1800):2383–2410

Pearson DG, Wittig N (2008) Formation of Archaean continental lithosphere and its diamonds: the root of the problem. J Geol Soc 165:895–914

Pearson DG, Carlson RW, Shirey SB, Boyd FR, Nixon PH (1995) Stabilization of Archean lithospheric mantle—a Re-Os isotope study of peridotite xenoliths from the Kaapvaal craton. Earth Planet Sci Lett 134(3–4):341–357

Pearson DG, Canil D, Shirey SB (2003) Mantle sample included in volcanic rocks: xenoliths and diamonds. In: Carlson RW (ed) Treatise on geochemistry: the mantle and core, vol 2. Elsevier, Amsterdam, pp 171–276

Porcelli DR, Onions RK, Galer SJG, Cohen AS, Mattey DP (1992) Isotopic relationships of volatile and lithophile trace-elements in continental ultramafic xenoliths. Contrib Mineral Petrol 110(4):528–538

Raffone N, Chazot G, Pin C, Vannucci R, Zanetti A (2009) Metasomatism in the lithospheric mantle beneath Middle Atlas (Morocco) and the origin of Fe- and Mg-rich wehrlites. J Petrol 50(2):197–249

Richardson SH, Erlank AJ, Hart SR (1985) Kimberlite-borne garnet peridotite xenoliths from old enriched subcontinental lithosphere. Earth Planet Sci Lett 75(2–3):116–128

Roden MF, Irving AJ, Murthy VR (1988) Isotopic and trace-element composition of the upper mantle beneath a young continental rift—results from Kilbourne-Hole, New-Mexico. Geochim Cosmochim Acta 52(2):461–473

Rollinson H (1993) Using geochemical data: evaluation, presentation, interpretation, Pearson

Schmidberger SS, Simonetti A, Francis D (2001) Sr-Nd-Pb isotope systematics of mantle xenoliths from Somerset Island kimberlites: evidence for lithosphere stratification beneath Arctic Canada. Geochim Cosmochim Acta 65(22):4243–4255

Schmidberger SS, Simonetti A, Francis D, Gariepy C (2002) Probing Archean lithosphere using the Lu-Hf isotope systematics of peridotite xenoliths from Somerset Island kimberlites, Canada. Earth Planet Sci Lett 197(3–4):245–259

Schmidberger SS, Simonetti A, Francis D (2003) Small-scale Sr isotope investigation of clinopyroxenes from peridotite xenoliths by laser ablation MC-ICP-MS—implications for mantle metasomatism. Chem Geol 199(3–4):317–329

Simon NSC, Irvine GJ, Davies GR, Pearson DG, Carlson RW (2003) The origin of garnet and clinopyroxene in "depleted" Kaapvaal peridotites. Lithos 71(2–4):289–322

Simon NSC, Carlson RW, Pearson DG, Davies GR (2007) The origin and evolution of the Kaapvaal cratonic lithospheric mantle. J Petrol 48(3):589–625

Sneeringer M, Hart SR, Shimizu N (1984) Strontium and samarium diffusion in diopside. Geochim Cosmochim Acta 48(8): 1589–1608

Stosch HG, Lugmair GW (1986) Trace-element and Sr and Nd isotope geochemistry of peridotite xenoliths from the Eifel (West-Germany) and their bearing on the evolution of the subcontinental lithosphere. Earth Planet Sci Lett 80(3–4):281–298

Tang QS, Chen L (2008) Structure of the crust and uppermost mantle of the Yanshan Belt and adjacent regions at the northeastern boundary of the North China Craton from Rayleigh wave dispersion analysis. Tectonophysics 455(1–4):43–52

Teixell A, Ayarza P, Zeyen H, Fernandez M, Arboleya ML (2005) Effects of mantle upwelling in a compressional setting: the Atlas Mountains of Morocco. Terra Nova 17(5):456–461

Thirlwall M (1991) Long term reproducibility of multicollector Sr and Nd ratio analyses. Chem Geol (Isotope Science Section) 94:85–104

Urchulutegui JF, Fernandez M, Zeyen H (2006) Lithospheric structure in the Atlantic-Mediterranean transition zone (southern Spain, northern Morocco): a simple approach from regional elevation and geoid data. Comptes Rendus Geosci 338(1–2): 140–151

van Achterbergh E, Griffin WL, Stiefenhofer J (2001) Metasomatism in mantle xenoliths from the Letlhakane kimberlites: estimation of element fluxes. Contrib Mineral Petrol 141(4):397–414

Walter MJ (1998) Melting of garnet peridotite and the origin of komatiite and depleted lithosphere. J Petrol 39(1):29–60

Witt-Eickschen G, Seck HA, Mezger K, Eggins SM, Altherr R (2003) Lithospheric mantle evolution beneath the Eifel (Germany): constraints from Sr-Nd-Pb isotopes and trace element abundances in spinel peridotite and pyroxenite xenoliths. J Petrol 44(6):1077–1095

Wittig N (2006) Application of novel U-Th-Pb and Lu-Hf techniques to tracing the melting and metsomatic history of mantle rocks. In: Danish Lithosphere Centre, vol PhD. University of Copenhagen, Copenhagen, p 351

Wittig N, Pearson DG, Baker J, Duggen S, Hoernle K (2008) Evidence for young carbonatitic metasomatism in the continental mantle root beneath the Middle Atlas, Morocco. In: 9th International kimberlite conference extended abstract volume

Wittig N, Pearson DG, Baker J, Duggen S, Hoernle K (2010a) A major element, PGE and Re–Os isotope study of Middle Atlas (Morocco) peridotite xenoliths: evidence for coupled introduction of metasomatic sulphides and clinopyroxene. Lithos 115(1–4):15–26

Wittig N, Pearson DG, Baker J, Duggen S, Hoernle K (2010b) Tracing the metasomatic and magmatic evolution of continental mantle roots with Sr, Nd, Hf and Pb isotopes: a case study of Middle Atlas (Morocco) peridotite xenoliths. Geochim Cosmochim Acta 74(4):1417–1435

Xu YG, Blusztajn J, Ma JL, Suzuki K, Liu JF, Hart SR (2008) Late Archean to early proterozoic lithospheric mantle beneath the western North China craton: Sr-Nd-Os isotopes of peridotite xenoliths from Yangyuan and Fansi. Lithos 102(1–2):25–42

Yaxley GM, Kamenetsky V, Green DH, Falloon TJ (1997) Glasses in mantle xenoliths from western Victoria, Australia, and their relevance to mantle processes. Earth Planet Sci Lett 148(3–4): 433–446